https://doi.org/10.3311/PPch.43431

Periodica Polytechnica Chemical Engineering

Enhancing Silica Extraction from Rice Husk Ash Using Acid Solvent and Polyethylene Glycol-400: Efficiency and Mechanism

Leny Yuliatun[1*], Mariyam Mariyam[2**], Lia Destiarti[3], Tri Windarti[4], Dita Ariyanti[5], Erlin Purwita Sari[6], Hidayatul Fajri MS[7], Nuzul Ficky Nuswantoro[1]

[1] Research Center for Biomass and Bioproducts, National Research and Innovation Agency, Serpong, 15314 South Tangerang, Banten, Indonesia
[2] Department of Chemistry, Faculty of Science, Institut Teknologi Sumatera, Jati Agung, 35365 Lampung, Indonesia
[3] Department of Chemistry, Faculty of Mathematics and Natural Sciences, Universitas Tanjungpura, 78114 Pontianak, Indonesia
[4] Chemistry Department, Faculty of Sciences and Mathematics, Universitas Diponegoro, 50275 Semarang, Indonesia
[5] Research Center for Applied Microbiology, National Research and Innovation Agency, 16911 Cibinong, Indonesia
[6] Directorate of Laboratory Management, Research Facilities, and Science, and Technology Park, National Research and Innovation Agency, 55281 Yogyakarta, Indonesia
[7] Biomedic Research Center, National Research and Innovation Agency, 16911 Cibinong, Indonesia
* Corresponding author, e-mail: leny004@brin.go.id
**Corresponding author, e-mail: mariyam@ki.itera.ac.id

Received: 26 January 2026, Accepted: 08 June 2026, Published online: 21 September 2026

Abstract

Silica derived from agricultural waste offers a sustainable pathway for producing advanced biomaterials, however, precise control over purity, structure, and morphology remains a challenge for dental applications. This study systematically investigates the effects of acidic solvent and polyethylene glycol-400 (PEG-400) concentration on the physicochemical properties of silica synthesized from rice husk ash (RHA). Silica was prepared via sol–gel route using NaOH, followed by acid neutralization with hydrochloric acid, sulfuric acid, or nitric acid. To tailor structural and morphological features, PEG-400 was introduced as a structure-directing agent at silica-to-PEG mass ratios of 1:1, 1:3, 1:5, and 1:7. Among the investigated acids, HCl treatment produced high-purity (99.4 wt%) amorphous silica, characterized by silanol (Si–OH) and siloxane (Si–O–Si) functional groups as confirmed by FTIR. Incorporation of PEG-400 at a 1:1 ratio induced the formation of a hybrid amorphous–crystalline phase, including cristobalite and tridymite while maintaining a high silica content (99.06 wt%). Morphological analysis revealed that the optimized PEG-400 concentration promoted uniform block-like agglomerates with enhanced structural homogeneity, attributed to controlled polymer–silica interactions during gelation. These findings demonstrate that synergistic HCl extraction and PEG-400 modification enable tunable control over silica phase composition and morphology, demonstrating RHA-derived silica as a promising candidate for next-generation dental biomaterials.

Keywords

silica, rice husk ash (RHA), HCl, PEG-400, crystallinity

1 Introduction

Silica (SiO_2) is abundantly present in agricultural wastes such as rice husks and constitutes a critical component in endodontic root canal filling materials due to its cement-like physicochemical behavior. Effective silica extraction from rice husks is typically achieved through controlled calcination within the temperature range of 700 °C–900 °C, yielding a high-purity silica. Previous studies reported silica purities of 98.7% and 98.9% at calcination temperatures of 700 °C and 800 °C, respectively [1]. Both calcination temperature and duration of the ashing process influence the structural order and crystallinity of the extracted silica. Notably, a temperature of approximately 700 °C represents the critical threshold at which silica undergoes a phase transition from an amorphous to a crystalline state [2]. The choice between amorphous and crystalline silica phases depends on the targeted application of the material. The selection of amorphous or crystalline silica is therefore application-dependent, as each

Cite this article as: Yuliatun, L., Mariyam, M., Destiarti, L., Windarti, T., Ariyanti, D., Sari, E. P., Fajri MS, H., Nuswantoro, N. F. "Enhancing Silica Extraction from Rice Husk Ash Using Acid Solvent and Polyethylene Glycol-400: Efficiency and Mechanism", Periodica Polytechnica Chemical Engineering, 2026. https://doi.org/10.3311/PPch.43431

phase exhibits distinct physicochemical properties that influence its performance in specific material systems.

Several synthesis methods have been developed to tailor the physicochemical properties of silica from rice husks, among which the sol-gel method is recognized as one of the most effective approaches. This method enables the synthesis of silica with purities exceeding 90% while offering superior control over composition, structure, and morphology [3, 4]. In a typical sol–gel process, a strong alkali such as sodium hydroxide is employed to dissolve silica from rice husk ash, forming a sodium silicate precursor solution [5]. Numerous studies have reported the synthesis of silica from rice husk ash using acid treatments, including nitric acid, sulfuric acid, and hydrochloric acid [3]. Oli et al. investigated the optimization of silica extraction from rice husk ash HCl, achieving silica content ranging from 85% to 99.1%, and demonstrated superior performance compared to conventional methods, with yields exceeding those reported for alkali hydrothermal extraction (52.8%) and approaching the optimized range of acid leaching processes (70–90%) [6]. The highest silica content from rice husk ash was also obtained using the sol-gel method with 1 M nitric acid of 99.87% on IR-64 type rice husk with a calcination temperature of 700 °C for 1 h [7]. Silica synthesis from rice husk ash (RHA) using H_2SO_4 has been reported to yield high purity levels, reaching 99.4% from bottom ash (95.10% RHA) and 99.3% from fly ash (80.20% RHA), with only trace impurities such as ZrO_2, CuO, and ZnO [8]. Furthermore, thermal extraction methods for rice husk ash have been reported to yield silica with purity up to 99.3%, while the alkali extraction method followed by precipitation using H_2SO_4 at pH 2, combined with furnace-assisted chemical treatment, produces the smallest particle size compared to other methods [9].

Additionally, acids such HNO_3, H_2SO_4, and HCl are used during sodium silicate gel deposition, influencing silica content and material properties by dissolving impurities like MgO, K_2O, and CaO. The structural phase and particle size distribution of the resulting silica are key determinants of its suitability for endodontic applications, with nanoscale silica being particularly desirable due to its high specific surface area and enhanced potential for bioactivity. Furthermore, incorporation of polymeric additives such as polyethylene glycol can further modulate the silica matrix, promoting improved structural organization and particle uniformity.

Polyethylene glycol (PEG) is a hydrophilic polymer with a high density of ether oxygen groups that facilitates extensive hydrogen bonding, enabling it to act as an efficient templating and structure-directing agent in silica synthesis for controlling particle morphology, size distribution, and pore architecture. During the sol–gel process, PEG interacts with silica precursors, altering hydrolysis, condensation, and gelation kinetics, thereby enabling controlled nucleation, growth, and assembly of silica nanoparticles [9]. Among its variants, PEG-400 (a low molecular weight grade) is commonly utilized in pharmaceutical formulations to enhance drug solubility and dissolution rates in aqueous media, as well as to improve drug biodistribution. In addition, PEG-400 may functions as a self-curing agent, contributing to the mechanical and handling properties of composite materials [10, 11]. The dual role of PEG-400 as both a structure-directing agent in silica synthesis and a functional excipient in drug delivery highlights its versatility and significance in the development of advanced biomaterials, including dental material applications.

PEG is a versatile polymer widely used in nanomaterial synthesis to control particle size and morphology. PEG-400 and PEG-4000 differ significantly in molar mass and physical properties; PEG-400 possesses a relatively low molar mass (~400 g mol^{-1}) with shorter polymer chains and exists as a liquid at room temperature, whereas PEG-4000 has a higher molar mass (~4000 g mol^{-1}) and typically exhibits a solid or semi-solid state. The shorter chain of PEG-400 allows for more effective intercalation within polymeric chains during material synthesis, providing better plasticizing and templating effects for producing smaller and more uniform silica nanoparticles. Consequently, PEG-400 is frequently utilized in sol-gel synthesis routes of silica from natural sources, where the PEG-to-silica ratio plays a critical role in controlling particle size, morphology, and agglomeration behavior [12]. Previous investigations indicate that a silica-to-PEG mass ratio of 1:3 achieves optimal particle characteristics for applications in dental root canal materials [13]. Moreover, PEG acts as an anticoagulant surfactant, stabilizing particle dispersion during synthesis [14, 15]. These attributes highlight PEG-400's importance in tailoring the physicochemical properties of silica-based biomaterials.

The synthesized silica from RHA exhibits significant potential for application in dental materials, particularly in endodontic treatment. This is attributed to the requirement that dental material components possess heterogeneous particle sizes to enable effective interlocking between fine silica particles and larger calcium-based particles, thereby enhancing mechanical strength and structural

integrity [16]. Beyond dental applications, RHA-derived silica has been widely explored in healthcare and biomedical fields. For instance, mesoporous RHA silica has been utilized in pharmaceutical applications as a drug delivery system due to its high adsorption capacity [17]. Additionally, silica serves as a reinforcing filler in biomedical rubber and dental products [18–21]. Other notable applications include its use in the synthesis of adsorbents, bioactive glass, and high-purity biocompatible silica-based materials [22–25]. Furthermore, silica has been incorporated into antimicrobial bio composite films, particularly for food packaging applications, where it enhances mechanical strength and functional performance [26, 27].

This study presents a comparative evaluation of the effects of three different strong acids solvents: HCl, H_2SO_4, HNO_3 under identical synthesis conditions to determine their effectiveness in producing silica from rice husk ash. Furthermore, this study extends beyond the extraction stage by investigating the role of PEG-400 as an organic templating agent in the silica sample extracted using the most effective solvent (HCl). Various PEG-400-to-silica mass ratios (1:1, 1:3, 1:5, and 1:7) were systematically examined to elucidate their influence on the structural and morphological properties of the synthesized silica. Silica extraction from RHA generally involves alkaline treatment using sodium hydroxide to form sodium silicate solution, followed by acid-induced gelation to precipitate silica gel. Prior research has demonstrated that HCl–mediated acidification produces silica with the highest purity and largest surface area, favoring the formation of amorphous silica characterized by extensive Si–O–Si bonding vibration as confirmed by Fourier transform infrared (FTIR) and X-ray diffraction (XRD) analyses. In this work, PEG-400 is employed as a templating agent in different ratios to tailor particle size, morphology, and crystallinity of the resulting silica. Optimizing the acid type and PEG-400 concentration ratio is important for producing silica with properties suitable for endodontic root canal applications. Accordingly, this study aims to identify the optimal acid–PEG-400 combination for generating high-quality silica precursors for advanced biomedical applications.

2 Materials and methods

2.1 Materials and instrumentations

All reagents and materials were purchased from reputable suppliers (Merck/Sigma-Aldrich or equivalent), with stated purities of 99% or higher unless otherwise specified. Chemicals included sodium hydroxide (≥99%), hydrochloric acid (37%), sulfuric acid (98%), nitric acid (65%), and polyethylene glycol 400. Deionized water with a resistivity of ≥18.2 MΩ cm was used throughout all experimental procedures. The commercial silica with ≥99% purity (Merck) was used as a reference material to ensure consistent composition, and all chemicals were properly stored and labeled to prevent contamination and ensure traceability.

Comprehensive characterizations of the synthesized silica were performed using X-ray fluorescence (XRF, RIGAKU NEX QC+QuanTEZ, Japan) to quantify elemental composition, Fourier Transform Infrared Spectroscopy (FTIR, 8201PC Shimadzu, Japan) to identify siloxane (Si–O–Si) and silanol (Si–OH) functional groups, X-ray diffraction (XRD, BRUKER AXS D8 Advance ECO, Germany; Cu-Kα, 40 kV, 25 mA) to assess crystallinity and phase purity, scanning electron microscopy coupled with energy-dispersive X-ray spectroscopy (SEM-EDX, JSM-6510OLA, Japan) for morphology and elemental mapping. The combined data confirmed high-purity silica with a predominantly amorphous structure, uniform morphology, and minimal residual carbon or metallic contaminants. The described methodology provides a scalable framework for converting rice husk waste into value-added silica while enabling consistent quality control across batches.

2.2 Synthesis and PEG-400 treatment of silica

Silica was synthesized from RHA via a sol-gel method. 10 g of RHA was dispersed in 60 mL of 2 M NaOH and heated to 80 °C for 60 min under continuous stirring to promote dissolution of silica and formation of soluble silicate species. The resulting suspension was subjected to a second extraction using an additional 30 mL of 2 M NaOH to maximize sodium silicate yield. The resulting extracts were combined and allowed to cool to room temperature.

The two extracts were combined and gradually titrated with variations acid (HCl, H_2SO_4, and HNO_3) until the pH reached neutrality, resulting in the formation of a silica wet gel. The gel was filtered and washed with distilled water (approximately 500 mL) to remove residual alkali and soluble impurities, until the filtrate pH approached neutral. The wet gel was oven-dried at 120 °C for 4 h to remove residual water, followed by calcination at 400 °C for 1 h to remove organics and improve porosity. The obtained silica powder was subsequently ground and sieved through a 200-mesh sieve (74 μm).

To obtain smaller and partially crystalline silica particles, the silica obtained using HCl as the acid precipitant

was further treated with PEG-400. PEG-400 was melted at 105 °C for 30 min and then mixed with the HCl-derived silica at silica-to-PEG-400 ratios of 1:1, 1:3, 1:5, and 1:7 mass/volume (w/v). Distilled water was added to the mixture solution with a PEG-to-water ratio of 1:2 (v/v) followed by stirring for 15 min. The resulting suspension was subjected to ultrasonic treatment for 60 min and oven at 105 °C for 24 h then aged under ambient conditions for an additional 48 h to facilitate structural stabilization. Finally, the dried samples were calcined at 750 °C for 1 h to remove the polymer (PEG-400) template. The structural, chemical, and morphological properties of the synthesized silica were characterized using XRD, FTIR, SEM, and EDX analyses.

3 Results and discussion

3.1 X-ray diffraction analysis of silica

XRD analysis of silica synthesized from rice husk ash (RHA) using different acid precipitants (HCl, HNO_3 and H_2SO_4) are presented in Fig. 1.

The XRD analysis reveals that silica precipitated from rice husk ash exhibits predominantly amorphous structure. Specifically, broad diffraction pattern near $2\theta \approx 22°$ confirms the dominance of amorphous silica [28]. The extent of peak broadening is markedly influenced by the sulfuric acid medium, producing the most pronounced amorphous phase [29–31]. The type of acid used during synthesis controls how silica units connect and organize, which in turn affects the material's strength and its ability to release biologically relevant ions in endodontic applications. HCl is a better solvent to use in precipitating silica from rice husk ash with high purity [3]. The incorporation of PEG-400 resulted in sharper and more intense diffraction peaks in the XRD patterns, indicating enhanced crystallinity and increased crystallite size. This behavior is attributed to improved dispersion of silicate species during gel formation and defect reduction during high-temperature calcination, which collectively promote crystal growth and long-range structural ordering [32]. The results of XRD analysis of variations in the use of PEG-400 from the HCl solvent can be seen in Fig. 2. Peak interpretations and quantitative metrics are summarized in Table 1.

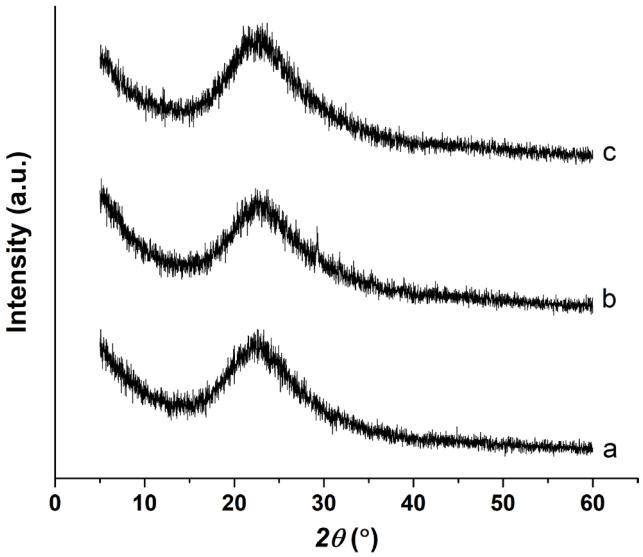

Fig. 1 XRD patterns of silica synthesized from rice husk ash using different acid precipitants: (a) hydrochloric acid, (b) nitric acid, and (c) sulfuric acid

Table 1 and Fig. 2 show that the silica precipitated from rice husk ash exhibits predominantly crystalline features at specific 2θ positions around 21.9°, 31.4°, and 36.0°, with additional reflections near 28.32° and 28.87° indicating a coexisting amorphous silica fraction embedded within a crystalline matrix. The presence of crystalline phases corresponds to silica polymorphs that may evolve with thermal treatment, in agreement with reported phase transitions of silica under heat [32]. Calcination at elevated temperatures may induce transformations among amorphous

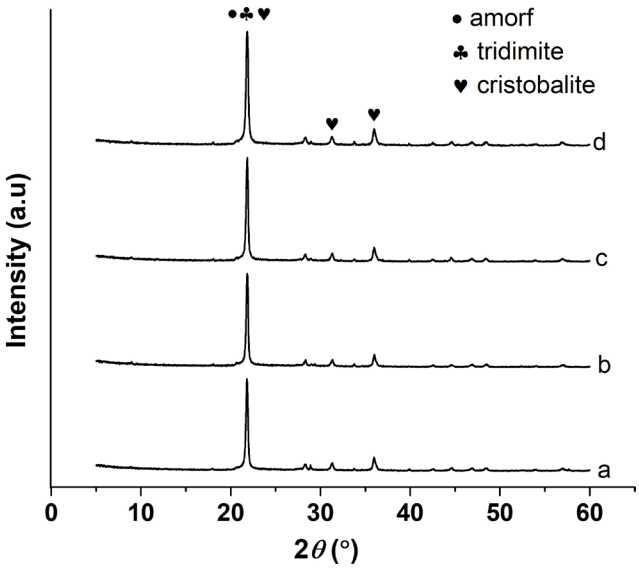

Fig. 2 Diffractogram of rice husk ash silica-to-PEG mass ratios of (a) 1:1, (b) 1:3, (c) 1:5, and (d) 1:7

Tabel 1 Peak from diffractogram RHA silica with PEG-400 template

Number	Peak 2θ (°)	Phase interpretation
1	21.82–21.90	Amorphous, tridymite, cristobalite
2	35.95–36.00	Cristobalite
3	31.24–31.39	Cristobalite
4	28.32–32.36	Quartz, amorphous
5	28.87	Quartz, amorphous

silica, and crystalline polymorphs such as cristobalite, and tridymite. Cristobalite typically forms at higher calcination temperatures and is associated with the sharpening of X-ray diffraction peaks, reflecting increased crystallite size and enhanced long-range ordering, whereas tridymite may remain stable over a broader temperature range [33]. Characteristic sharp reflections attributable to crystalline quartz, when present, are observed at 2θ values of approximately 20.77°, 26.62°, 50.26°, 60.02°, and 68.27°, whereas the broad feature (hump) at low angles remains indicative of amorphous silica. The reported slight shifts toward higher 2θ at high calcination temperatures are consistent with lattice parameter changes associated with crystallite growth and structural reorganization. In contrast, an intense and broad peak near $2\theta \approx 22°$ is often associated with amorphous silica. This amorphous characteristics can be further influenced by templating agents such as PEG-400, which modulate particle size and degree of polymerization during gel formation, thereby affecting the final phase distribution [34, 35]. Overall, the data indicates a solvent- and template-dependent balance between amorphous and crystalline silica phases, wherein higher calcination temperatures promote crystallite growth and the development of mixed-phase structures that may either enhance or compromise functional properties relevant to endodontic applications.

3.2 Silica functional groups with Fourier transform infrared spectroscopy

FTIR spectroscopy was employed to analyze the functional groups present in silica derived from rice husk ash precipitated using different acids, as shown in Fig. 3. The band observed at approximately 470 cm^{-1} corresponds to the bending vibration of ≡Si–O–Si≡ (siloxane). The absorption near 790 cm^{-1} is assigned to the symmetric stretching vibration of ≡Si–O–Si≡, which shows a slight shift from the typical value of ~802 cm^{-1}. The strong band at around 1095 cm^{-1} is attributed to the asymmetric stretching vibration of siloxane groups, shifted from the standard ~1100 cm^{-1} position. The absorption at 1635 cm^{-1} is associated with the bending vibration of molecularly adsorbed water, while the broad band centered at approximately 3448 cm^{-1} corresponds to the stretching vibrations of hydrogen-bonded Si−OH and O−H of surface-adsorbed water. Additionally, a band at approximately 2368 cm^{-1} is observed and is commonly attributed to adsorbed CO_2 from the atmosphere. A weak band near 3749 cm^{-1} is assigned to isolated silanol (Si–OH) stretching vibrations.

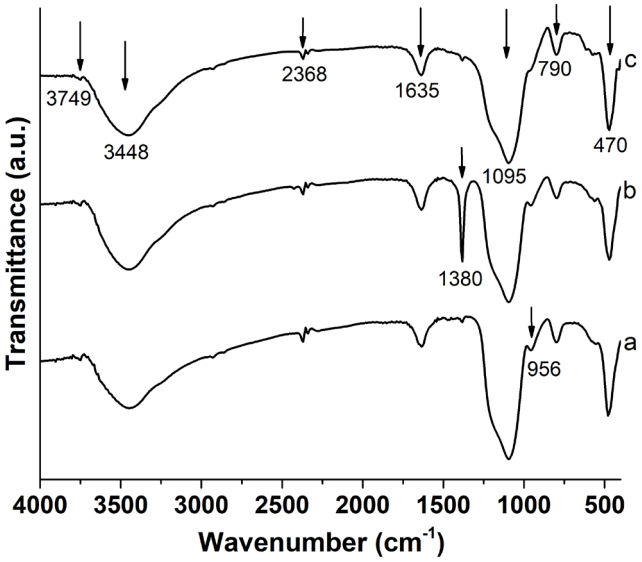

Fig. 3 FTIR spectra of silica synthesized from rice husk ash using different acid precipitants: (a) HCl, (b) HNO_3, and (c) H_2SO_4, where the arrows indicate the characteristic peaks, along with their corresponding wavenumbers, on the respective bands

Notably, silica samples synthesized using HCl and HNO_3 exhibit an additional weak absorption band near 956 cm^{-1}, which is assigned to the stretching vibration of ≡Si–OH groups, a characteristic feature of silica gel structures [12]. In contrast, silica prepared using HNO_3 shows a distinct and sharp absorption band at approximately 1380 cm^{-1}, corresponding to N–O stretching vibrations of residual nitrate (NO_3^-) species originating from the nitric acid solvent. The presence of this band indicates incomplete removal or incorporation of nitrate species within the silica matrix. FTIR analysis confirms that all three acid solvents are capable of producing silica; however, HCl is identified as the most suitable precipitating agent due to the absence of nitrate-related impurities, higher chemical purity, and the pronounced presence of siloxane (≡Si–O–Si≡) functional groups. Furthermore, RHA-derived silica synthesized using HCl in combination with PEG-400 exhibits the infrared spectrum shown in Fig. 4, with detailed functional group assignments summarized in Table 2.

The FTIR data presented in Table 2 confirm the presence of characteristic silanol and siloxane functional groups, as evidenced by the corresponding Si–O vibrational modes. Additionally, the detection of an intermolecular forces (hydrogen-bonded Si–OH) at 3448 cm^{-1} further supports the successful formation of silica. Distinct absorption bands at 468, 617, 794, 1095, and 3448 cm^{-1} are consistent with the typical vibrational features of silica materials. Among the samples analyzed, the RHA–PEG-400 silica composite prepared at a silica-to-PEG

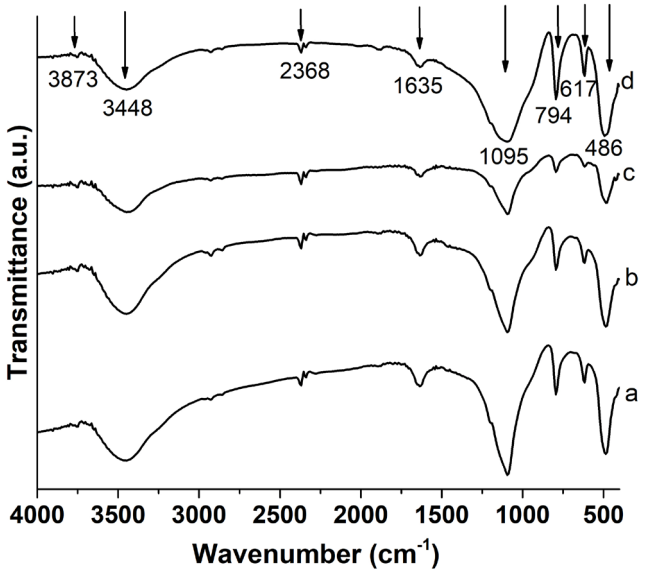

Fig. 4 FTIR spectra of RHA silica after calcination at 750 °C with varying silica-to-PEG ratios of (a) 1:1, (b) 1:3, (c) 1:5, and (d) 1:7, where the arrows indicate the characteristic peaks, along with their corresponding wavenumbers, on the respective bands

Table 2 Assignation of the FTIR signals of RHA silica with HCl and PEG-400

Number	Wavenumber (cm^{-1})	Functional group
1	486	Stretching vibration of ≡Si–O–Si≡
2	617	Stretching vibration of Si–O from ≡Si–O–Si≡
3	794	Symmetric stretching vibration of Si–O from ≡Si–O–Si≡
4	1095	Asymmetric stretching vibration of Si–O from ≡Si–O–Si≡
5	1635	Bending vibration of –OH from H_2O
6	2368	Stretching vibration of Si–O from ≡Si–O–Si≡
7	3448	Stretching vibration of –OH from H_2O and –OH from Si–OH (hydrogen bonded)
8	3873	Stretching vibration of –OH from H_2O

ratio of 1:5 exhibits the lowest overall absorption intensity. The emergence of a band at 2854 cm^{-1} in samples with RHA–PEG-400 ratios of 1:3, 1:5, and 1:7—compared to 2862 cm^{-1} at a 1:1 ratio—reflects a redshift, indicating an elongation of hydrogen bonds. This shift is likely due to the combined effects of calcination temperature and the presence of PEG-400, a long-chain polymer that modifies the silica network [36]. Moreover, decreasing the PEG-400 content (1:1 ratio) results in increased hygroscopicity and hydrophilicity, as demonstrated by the broadening of the absorption band at 3448 cm^{-1}. These findings highlight the influence of PEG-400 concentration and calcination on the structural and surface properties of the synthesized silica, providing insight into the hydrogen-bonding dynamics and hydrophilic character of the material.

Typically, the presence PEG is indicated by characteristic FTIR bands at around 1460 cm^{-1} and 2950–2800 cm^{-1}, corresponding to the bending and stretching vibrations of CH_2 respectively [37]. In this study the FTIR spectra of PEG-assisted samples after calcination show a substantial reduction in the C–H-related vibrational bands, indicating that PEG-400 was mostly removed at 750 °C, although weak residual band at 2950–2800 cm^{-1} may still remain [37]. Preliminary study indicates that PEG-400 decomposes predominantly below ~450 °C. Therefore, it is plausible that calcination at lower temperatures (e.g., 500–600 °C) may already be sufficient to remove most of the PEG template while potentially minimizing the risk of structural densification or partial crystallization of silica at higher temperatures [38]. Moreover, a sharper and more intense Si–O–Si asymmetric stretching band (~1095 cm^{-1}) on silica synthesized with PEG-400 (1:1 ratio) is observed compared to silica synthesized without PEG-400, indicating improved structural organization and densification.

Although PEG-400 is predominantly removed during calcination at 750 °C, as evidenced by the very weak intensity of the C–H-related bands in the FTIR spectra, its presence during the pre-calcination stage still played an important role in determining the final silica structure. PEG-400 acts as a structure-directing agent, facilitating the spatial organization of silicate species through polymer–silica interactions [38]. Upon thermal treatment, the decomposition of PEG-400 is accompanied by densification and structural rearrangement, resulting in the formation of more defined, crystalline-like silica domains which is consistent with SEM observations, where PEG-assisted samples exhibit clearer interparticle boundaries and more ordered geometries, rather than reduced particle size or suppressed agglomeration (Fig. 6). These findings indicate that PEG-400 primarily contributes to structural evolution and particle reorganization. Such behavior has been widely reported in polymer-assisted sol–gel systems, where organic templates are thermally removed but leave a persistent impact on the final material architecture.

3.3 Oxide component of silica

The elemental and oxide composition of the synthesized silica was analyzed using EDX, which was coupled with SEM to simultaneously provide compositional and morphological information. EDX analysis enables the

identification and semi-quantitative determination of constituent elements and their corresponding oxide forms, thereby allowing assessment of silica purity and the presence of residual inorganic impurities.

Analysis of the data in Table 3 shows that silica yield is maximized when nitric acid is used as the solvent, reaching 0.11%, which is higher than the yields obtained using hydrochloric acid (HCl) and sulfuric acid. This observation is consistent with previous reports in the literature [22, 39]. The calcination temperature range of 700–750 °C was chosen to ensure effective removal of organic components and other impurities while maintaining silica predominantly in the amorphous phase. The full crystallization of silica into phases such as tridymite and cristobalite typically occurs at temperatures above 1000 °C [40]. In terms of chemical purity, silica samples synthesized using HNO_3 and HCl exhibit the highest silica content among the investigated solvents. The solvent choice should be tailored to the intended end use of the raw material in endodontic dentistry, where heterogeneous particle size distributions can enhance packing density, compressive strength, and scaffold integrity of cementitious systems [41]. Additionally, quantification of oxide content in rice husk ash silica prepared with HCl and PEG-400 is summarized in Table 4.

As shown in Table 4, silica derived from RHA via the sol–gel process achieves near-pure SiO_2 composition when synthesized at an RHA:PEG-400 ratio of 1:1, yielding a maximum SiO_2 content of 99.06%. The minor carbon contamination from the PEG-400, contributes to high silica purity. Minor oxide impurities originating from the rice husk ash, such as CaO, CuO, and ZnO, remain present at low concentrations and can influence the final compositional balance of the silica. These secondary oxides have been reported to act as reinforcing constituents in cementitious systems, potentially enhancing compressive strength and structural stability in endodontic materials [3]. The compositional data in Table 4 suggest that these non-silica constituents can function as reinforcing phases to improve mechanical performance. Prior work reports an optimum silica:PEG ratio of 1:3 for balanced purity and reinforcement [13].

Table 3 Oxide components in silica from rice husk ash treated with various acid

Oxide	Acid		
	HCl (% mass)	HNO_3 (% mass)	H_2SO_4 (% mass)
SiO_2	99.40	99.51	93.10
K_2O	0.60	0.49	0.34
SO_3	-	-	6.56

Table 4 Oxide components in silica from rice husk ash synthesized using HCl and different PEG-400 concentrations

Ratios of silica: PEG-400	Oxide composition (wt%)						
	SiO_2	CaO	MnO	NiO	CuO	ZnO	SrO
1:1	99.06	0.79	0.09	0.02	0.01	0.01	0.01
1:3	97.55	2.31	0.09	0.02	0.01	0.01	0.01
1:5	98.99	0.92	0.09	0.02	0.01	0.01	<0.01
1:7	98.80	1.06	0.09	0.02	0.01	0.01	<0.01

3.4 Silica surface morphology

Acid selection plays a critical role in governing the morphology of silica precipitated from sodium silicate solutions derived from rice husk ash and NaOH [42]. SEM images (Fig. 5) show that silica prepared with HCl exhibits more heterogeneous morphology, including amorphous spheres and particle agglomeration [43]. In contrast, silica precipitated with H_2SO_4 appears clearer and well-defined geometrical features. Meanwhile, silica obtained using HNO_3 displays the smallest particle size at the same magnification, indicating a finer and more uniform particle distribution. Such small and uniform particles may reduce density and yield larger pore volumes. These results indicate that acid-driven control of nucleation and growth is a key parameter for tailoring porosity and density in rice husk–derived silica.

Based on SEM analysis of silica precipitated from a rice husk ash–NaOH system indicates that using HCl as the precipitating solvent produces surface morphologies that are particularly compatible with root canal material applications. The resulting silica exhibits dispersed particles with a broad size distribution and notable agglomeration. Such morphological heterogeneity allows interparticle packing that can fill micro-gaps and voids within the endodontic matrix, potentially enhancing both physical integrity and sealing capability. In comparison, silica prepared with other acids (e.g., H_2SO_4, HNO_3) displays more uniform or crystalline-like geometries, which may influence porosity and density differently. The PEG-400 modifier further modulates these morphologies, as evidenced by distinct surface features and agglomeration patterns in the PEG-containing systems. Overall, acid-mediated control of nucleation and growth governs the resulting surface topology and packing behavior, providing a rational basis for selecting synthesis conditions tailored to silica additives for endodontic applications.

SEM analysis presented in Fig. 6 reveals distinct morphological variations in silica precipitated from the rice

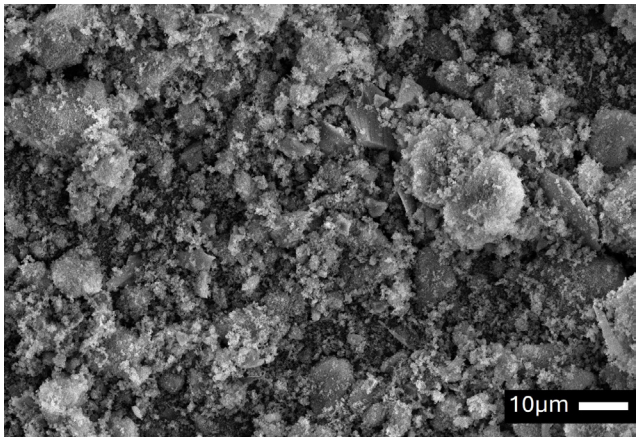

(a)

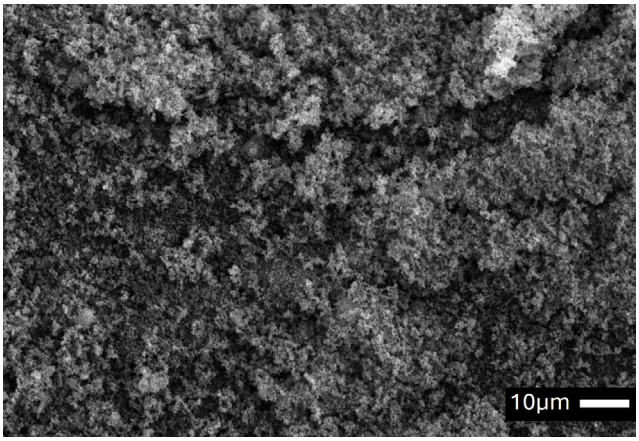

(b)

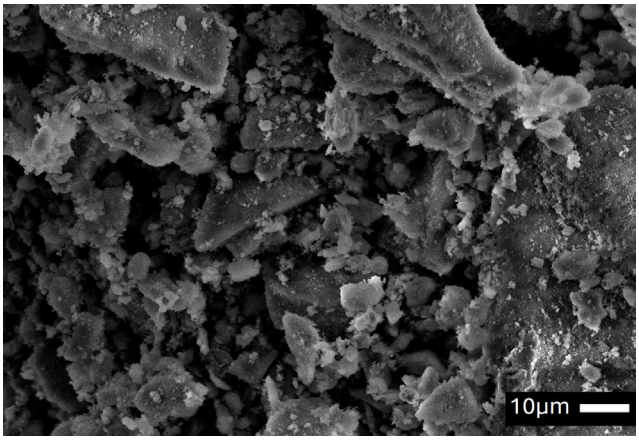

(c)

Fig. 5 SEM image of silica magnification 1000× with solvent (a) HCl, (b) HNO_3, (c) H_2SO_4

husk ash–NaOH system depending on PEG-400 templating and acid selection. At identical magnification (1000×), silica synthesized with HCl exhibits minimal agglomeration and a broad size distribution with noticeable interparticle packing, which is favorable for filling microvoids in root canal treatment. In contrast, silica prepared using other acids (H_2SO_4) tends toward more uniform, crystalline-like morphologies with reduced agglomeration, while silica synthesized with HNO_3 yields the smallest particle size under the same imaging conditions.

The presence of long, block-like needle features (red arrows in Fig. 6) in some samples indicates partial crystallinity within the silica framework, which can further affect packing efficiency and mechanical properties. Previous study investigated that silica synthesized with PEG-400 exhibits predominantly spherical particles that assemble into an interconnected porous structure with macroporous characteristics [44]. Further investigation using nitrogen adsorption–desorption analysis is necessary to quantitatively evaluate the evolution of the porous structure induced by different acid solvents and PEG-400 concentrations, as well as to confirm the structural stability of the pores after calcination at 750 °C. Overall, PEG-400 templating modulates dispersion and agglomeration, with 1:1 silica:PEG-400 ratios delivering a balanced morphology that supports effective packing and potential reinforcement in root canal applications [45].

Based on comprehensive multi-technique characterization (XRD, FTIR, and SEM-EDX), the preferred solvent for raw materials designed for endodontic applications is hydrochloric acid, yielding amorphous silica with purity approaching 99.4% and clear evidence of silanol and siloxane functionalities. SEM reveals heterogeneous particle agglomeration that can enhance packing and interfacial contact within a restorative matrix. When PEG-400 templating is employed, crystalline phases emerge, including cristobalite and tridymite, accompanied by uniform agglomeration sizes indicative of controlled crystallinity. The 1:1 silica to PEG-400 ratio shows an optimal balance of dispersion and controlled agglomeration, aligning with observed maximum silica content near 99.06%. These results reveal the ability to tailor structure and purity through solvent choice and templating, with direct implications for endodontic performance. The PEG-400 templating not only enables crystalline silica phases under certain conditions but also provides control over particle size distribution, enabling small, uniform particles that facilitate dense packing and reduced porosity gaps. Importantly, the silica to PEG-400 ratio of 1:1 achieves the highest silica content (~99.06%) while maintaining controlled agglomeration, indicating an optimal balance between chemical purity, morphological characteristics, and potential mechanical reinforcement.

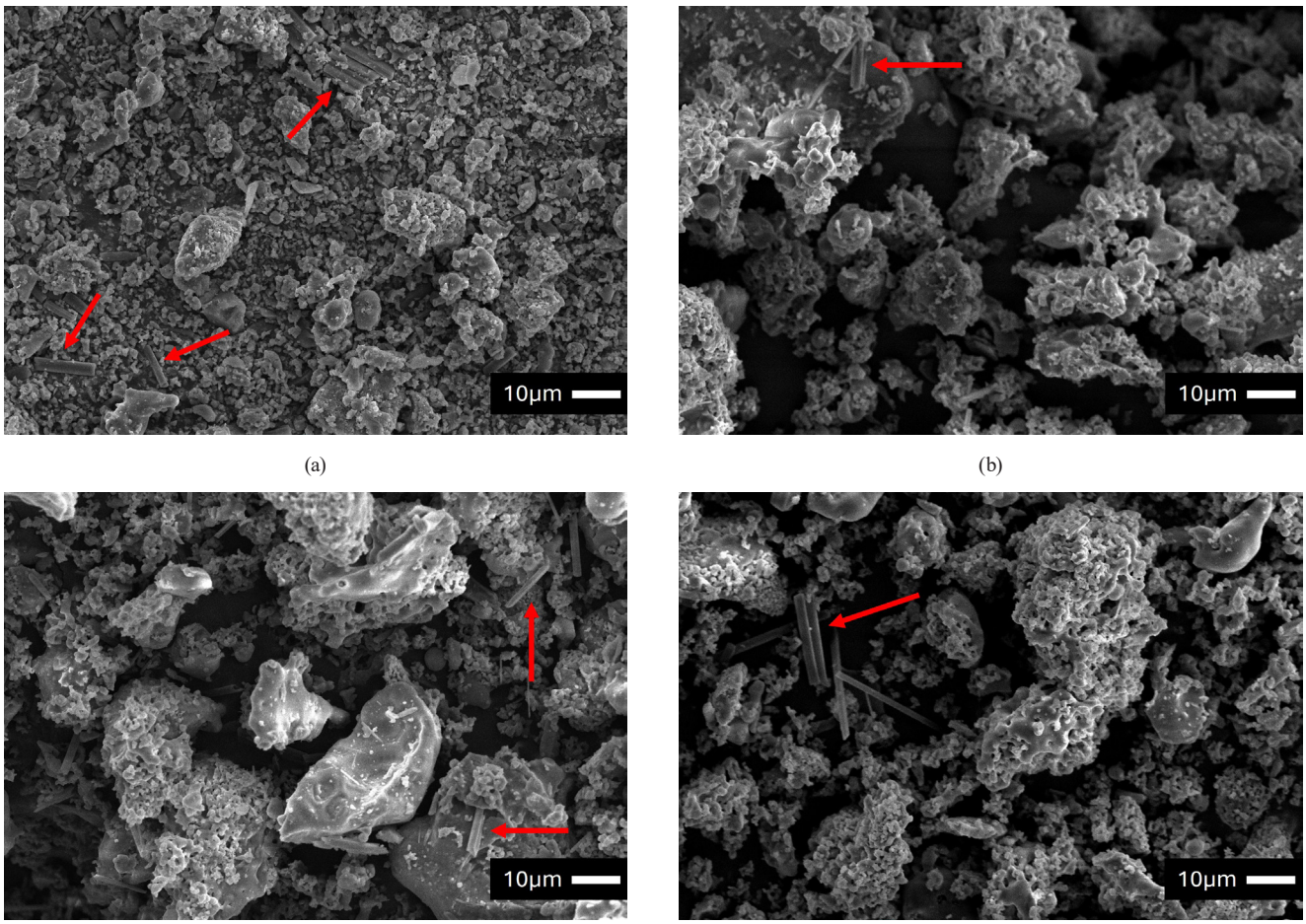

(a) (b)

(c) (d)

Fig. 6 SEM image magnification 1000× of samples with silica PEG-400 ratio (a) 1:1, (b) 1:3, (c) 1:5, (d) 1:7, where the red arrows show long, block-like needle features, indicating partial crystallinity within the silica framework.

4 Conclusions

Silica extraction from rice husk ash was significantly influenced by the type of acid treatment employed. Among the investigated acids, HCl provides superior structural development compared to H_2SO_4 and HNO_3, as evidenced by the more intense Si–O–Si vibrational band. The incorporation of PEG-400 as a structure-directing agent significantly affected the structural evolution of silica after calcination at 750 °C. The reduction of organic-related vibrational bands confirmed the substantial removal of PEG-400, accompanied by structural reorganization and densification of the silica framework. Among the investigated compositions, the PEG-400 ratio of 1:1 exhibited the most favorable structural characteristics. Although complete crystallization was not achieved, partial structural ordering and morphological development were observed.Overall, the combination of HCl-assisted extraction and PEG-400 templating provides a simple, effective, and potentially scalable strategy for producing biomass-derived silica with controllable structural characteristics, phase composition, and morphology. Furthermore, these findings establish a scalable and sustainable route for producing biomass-derived silica with controllable purity, phase composition, and morphology, offering potential properties for endodontic applications.

Acknowledgement

This research was funded by the Republic Indonesia Endowment Fund for Education (LPDP-RI) and the National Research and Innovation Agency (BRIN) through the RIIM Competition Batch 7 (2nd year), under Contract Nos. B-3871/II.7.5/KS.00/4/2025 and B-2599/III.10.FR.06.00/4/2025, and was supported in part by the Deputy for Research and Innovation Facilitation and Research Organization for Nanotechnology and Materials, National Research and Innovation Agency (BRIN), through a BRIN research grant in 2026.

References

[1] Fernandes, I. J., Calheiro, D., Sánchez, F. A. L., Camacho, A. L. D., de Campos Rocha, T. L. A., Moraes, C. A. M., de Sousa, V. C. "Characterization of silica produced from rice husk ash: Comparison of purification and processing methods", Materials Research 20(Suppl 2), pp. 512–518, 2017. https://doi.org/10.1590/1980-5373-mr-2016-1043

[2] Secundino-Sánchez, O., Diaz-Reyes, J., Sánchez-Ramírez, J. F., Jiménez-Pérez, J. L. "Structural and optical characterization of the crystalline phase transformation of electrospinning TiO_2 nanofibres by high temperatures annealing", Revista Mexicana de Fisica, 65(5), pp. 459–467, 2019. https://doi.org/10.31349/RevMexFis.65.459

[3] Nzereogu, P. U., Omah, A. D., Ezema, F. I., Iwuoha, E. I., Nwanya, A. C. "Silica extraction from rice husk: Comprehensive review and applications", Hybrid Advances, 4, 100111, 2023. https://doi.org/10.1016/j.hybadv.2023.100111

[4] Setyawan, N., Hoerudin, Yuliani, S. "Synthesis of silica from rice husk by sol-gel method", IOP Conference Series: Earth and Environmental Science, 733, 012149, 2021. https://doi.org/10.1088/1755-1315/733/1/012149

[5] Pipathworapoom, W., Hsu, H.-P., Manibalan, K., Lan, C.-W. "Rapid synthesis of sodium silicate through adiabatic reaction with low emission starting from exhausted KL-Si", Journal of Cleaner Production, 376, 134298, 2022. https://doi.org/10.1016/j.jclepro.2022.134298

[6] Oli, A., Swar, J., Sedhai, B., Sapkota, M. "Optimization of Silica Extraction Method from Rice Husk Ash Using Taguchi Method", [preprint] Preprints.org, 25 December 2025. https://doi.org/10.20944/preprints202512.2253.v1

[7] Mutrofin, S., Krisna, L., Mardiana, D., Tjahjanto, R. T. "Acid Isolation Techniques for Silica isolation from Rice Husk and Determination of Its Physicochemical Properties", The Journal of Pure and Applied Chemistry Research, 11(1), pp. 72–82, 2022. https://doi.org/10.21776/ub.jpacr.2022.011.01.641

[8] Molgamudi, S. P., Thogaru, S., Sutar, S. M. "High-Purity Silica Extraction from Rice Husk Ash via Optimized Biomass Gasification: A Comparative Study of Fly and Bottom Ash", Silicon, 17(17), pp. 4001–4012, 2025. https://doi.org/10.1007/s12633-025-03465-7

[9] Lavrova, D. G., Zvonarev, A. N., Alferov, V. A., Khonina, T. G., Shadrina, E. V., Alferov, S. V., Ponamoreva, O. N. "Biocompatible Silica-Polyethylene Glycol-Based Composites for Immobilization of Microbial Cells by Sol-Gel Synthesis", Polymers, 15(2), 458, 2023. https://doi.org/10.3390/polym15020458

[10] Sun, S., Cui, Y., Yuan, B., Dou, M., Wang, M., Xu, H., Wang, J., Yin, W., Wu, D., Peng, C. "Drug delivery systems based on polyethylene glycol hydrogels for enhanced bone regeneration", Frontiers in Bioengineering and Biotechnology, 11, 1117647, 2023. https://doi.org/10.3389/fbioe.2023.1117647

[11] Hamzah, N., Mohd Saman, H., Baghban, M. H., Mohd Sam, A. R., Faridmehr, I., Muhd Sidek, M. N., Benjeddou, O., Huseien, G. F. "A Review on the Use of Self-Curing Agents and Its Mechanism in High-Performance Cementitious Materials", Buildings, 12(2), 152, 2022. https://doi.org/10.3390/buildings12020152

[12] Mujiyanti, D. R., Saptarini, M. D., Emi, N. H., Santoso, U. T. "Synthesis and Characterization Nanosilica from Rice Husk Ash Using Sol-Gel Method with Addition Of PEG-6000 and PVA", JKPK (Jurnal Kimia Dan Pendidikan Kimia), 6(3), pp. 252–263, 2021. https://doi.org/10.20961/jkpk.v6i3.54320

[13] Maryudi, M., Rahayu, A., Hakika, D. C. "Effectiveness of polyethylene glycol-coated silica on ions adsorption in industrial wastewater", Polimery, 68(5), pp. 259–263, 2023. https://doi.org/10.14314/polimery.2023.5.2

[14] Sharma, A., Liu, N., Ma, Q., Zheng, H., Kawazoe, N., Chen, G., Yang, Y. "PEG assisted P/Ag/Ag_2O/Ag_3PO_4/TiO_2 photocatalyst with enhanced elimination of emerging organic pollutants in salinity condition under solar light illumination", Chemical Engineering Journal, 385, 123765, 2020. https://doi.org/10.1016/j.cej.2019.123765

[15] Mardiyanto, Fithri, N. A., Amriani, A., Herlina, Sari, D. P. "Formulation and characterization of glibenclamide solid lipid nanoparticles formatted by virgin coconut oil and solid matrix surfactant", Science and Technology Indonesia, 6(2), pp. 58–66, 2021. https://doi.org/10.26554/STI.2021.6.2.58-66

[16] Yuliatun, L., Lubis, M. A. R., Kusala, M. K. J., Destiarti, L., Betriani, R., Budiarta, J., Mariyam, M. "Radiographic, Mechanical, and Chemical Properties of Mineral Trioxide Aggregate from Nanosilica and Clam Shell Calcium Carbonate", 278, 117590, 2025. https://doi.org/10.1016/j.poly.2025.117590

[17] Benkő, F., Kristó, K., Sovány, T. "Mesoporous silica nanoparticles as drug delivery systems [abstract]", In: VI. Symposium of Young Researchers on Pharmaceutical Technology, Biotechnology and Regulatory Science, Szeged, Hungary, 2024, p. 59. https://doi.org/10.14232/syrptbrs.2024.59

[18] Hu, Y., Dai, B., Xu, Z., Chen, H., Lu, X. "Fumed silica filler reinforces adhesion between silicone rubber and solid aluminum substrate", Colloids and Surfaces A: Physicochemical and Engineering Aspects, 725, 137592, 2025. https://doi.org/10.1016/j.colsurfa.2025.137592

[19] Gao, G., Raja Awang, R. A., W Ahmad, W. M. A., Ismail, N. H. "Natural Silica and Plant-Derived Fillers for Dental Composite Resins: A Narrative Review", Cureus, 17(10), e94509, 2025. https://doi.org/10.7759/cureus.94509

[20] Mariyam, M., Sunarintyas, S., Yuliatun, L., Irnawati, D., Hatmanto, A. D., Nuryono, N. "Physicochemical and antibacterial properties of ZnO/chitosan-modified mineral trioxide aggregate composites", Case Studies in Chemical and Environmental Engineering, 9, 100749, 2024. https://doi.org/10.1016/j.cscee.2024.100749

[21] Yuliatun, L., Nuswantoro, N. F., Lubis, M. A. R., Betriani, R., Budiarta, J., Destiarti, L., Ariyanti, D., Sari, E. P., Mariyam, M. "Effect of calcination temperature on the preparation of mineral trioxide aggregate from nano silica and clam shells calcium carbonate for endodontic applications", Journal of the Australian Ceramic Society, 62(1), pp. 165–174, 2026. https://doi.org/10.1007/s41779-025-01244-6

[22] Nzereogu, P. U., Omah, A. D., Ezema, F. I., Iwuoha, E. I., Nwanya, A. C. "Silica extraction from rice husk: Comprehensive review and applications", Hybrid Advances, 4, 100111, 2023. https://doi.org/10.1016/j.hybadv.2023.100111

[23] Yuliatun, L., Mariyam, M., Rois, M. F., Destiarti, L., Ariyanti, D., Purwita Sari, E., Fajri MS, H., Ficky Nuswantoro, N., Hadiyawarman, H. "Development and Physicochemical Analysis of SrO/Hydroxyapatite Modified Mineral Trioxide Aggregate Synthesized from Calcium Carbonate and Tetraetyl Ortosilicate as an Endodontic Material", Periodica Polytechnica Chemical Engineering, 69(4), pp. 673–684, 2025. https://doi.org/10.3311/PPch.41048

[24] Kedjo, G. Y., Hatmanto, A. D., Irnawati, D., Pambudi, F. I., Mariyam, M., Nuryono, N. "Physicochemical and antibacterial properties of white mineral trioxide aggregate after replacement of Bi_2O_3 with ZnO nanoflowers", Materials Chemistry and Physics, 348, 131647, 2026. https://doi.org/10.1016/j.matchemphys.2025.131647

[25] Mariyam, M., Sunarintyas, S., Nuryono, N. "Improving mechanical, biological, and adhesive properties of synthesized mineral trioxide aggregate by adding chitosan", Inorganic Chemistry Communications, 149, 110446, 2023. https://doi.org/10.1016/j.inoche.2023.110446

[26] Suvarna, V., Nair, A., Mallya, R., Khan, T., Omri, A. "Antimicrobial Nanomaterials for Food Packaging", Antibiotics, 11(6), 729, 2022. https://doi.org/10.3390/antibiotics11060729

[27] Zhang, W., Ahari, H., Zhang, Z., Jafari, S. M. "Role of silica (SiO_2) nano/micro-particles in the functionality of degradable packaging films/coatings and their application in food preservation", Trends in Food Science & Technology, 133, pp. 75–86, 2023. https://doi.org/10.1016/j.tifs.2023.01.009

[28] Haider, J. B., Haque, M. I., Hoque, M., Hossen, M. M., Mottakin, M., Khaleque, M. A., Johir, M. A. H., Zhou, J. L., Ahmed, M. B., Zargar, M. "Efficient extraction of silica from openly burned rice husk ash as adsorbent for dye removal", Journal of Cleaner Production, 380, 135121, 2022. https://doi.org/10.1016/j.jclepro.2022.135121

[29] Sunarti, S., Mariwy, A., Laitupa, A. N. "Synthesis and Characterization of Silica Gel from Palm Shell and Coir Ash", Indonesian Journal of Chemical Research, 11(1), pp. 59–64, 2023. https://doi.org/10.30598//ijcr.2023.11-mar

[30] Ghadafi, M., Santosa, S. J., Kamiya, Y., Nuryono, N. "Free Na and Less Fe Compositions of SiO_2 Extracted from Rice Husk Ash as the Silica Source for Synthesis of White Mineral Trioxide Aggregate", Key Engineering Materials, 840, pp. 311–317, 2020. https://doi.org/10.4028/www.scientific.net/KEM.840.311

[31] Dhaneswara, D., Fatriansyah, J. F., Situmorang, F. W., Haqoh, A. N. "Synthesis of Amorphous Silica from Rice Husk Ash: Comparing HCl and CH_3COOH Acidification Methods and Various Alkaline Concentrations", International Journal of Technology, 11(1), pp. 200–208, 2020. https://doi.org/10.14716/ijtech.v11i1.3335

[32] Gupta, A., Pandey, V., Yadav, M. K., Mohanta, K., Majhi, M. R. "A comparative study on physio-mechanical properties of silica compacts fabricated using rice husk ash derived amorphous and crystalline silica", Ceramics International, 48(23), pp. 35750–35758, 2022. https://doi.org/10.1016/j.ceramint.2022.07.098

[33] Li, W., Xu, C., Xie, A., Chen, K., Yang, Y., Liu, L., Zhu, S. "Microstructure study of phase transformation of quartz in potassium silicate glass at 900 °C and 1000 °C", Crystals, 11(12), 1481, 2021. https://doi.org/10.3390/cryst11121481

[34] Eknapakul, T., Jiamprasertboon, A., Amonpattaratkit, P., Pimsawat, A., Daengsakul, S., …, Yimnirun, R. "Unraveling the structural complexity of and the effect of calcination temperature on calcium phosphates derived from Oreochromis niloticus bones", Heliyon, 10(8), e29665, 2024. https://doi.org/10.1016/j.heliyon.2024.e29665

[35] Saidani, A., Boudraa, R., Fendi, K., Benouadah, L., Benabbas, A., Djermoune, A., Salvestrini, S., Bollinger, J.-C., Alayyaf, A. A., Mouni, L. "Effect of Calcination Temperature on the Photocatalytic Activity of Precipitated ZnO Nanoparticles for the Degradation of Rhodamine B Under Different Light Sources", Water, 17(1), 32, 2025. https://doi.org/10.3390/w17010032

[36] Alaneme, K. K., Oke, S. R., Fagbayi, S. B., Alabi, O. O., Ojo, O. M., Kareem, S. A., Folorunso, D. O. "Synthesis and structural analysis of calcined poultry manure for hydroxyapatite development", Next Sustainability, 5, 100079, 2025. https://doi.org/10.1016/j.nxsust.2024.100079

[37] Akbari, A., Yegani, R., Pourabbas, B. "Synthesis of poly(ethylene glycol) (PEG) grafted silica nanoparticles with a minimum adhesion of proteins via one-pot one-step method", Colloids and Surfaces A: Physicochemical and Engineering Aspects, 484, pp. 206–215, 2015. https://doi.org/10.1016/j.colsurfa.2015.07.042

[38] Gorbunova, O. V., Baklanova, O. N., Gulyaeva, T. I. "Porous structure of PEG-mediated silica controlled by solution pH", Microporous and Mesoporous Materials, 307, 110468, 2020. https://doi.org/10.1016/j.micromeso.2020.110468

[39] Gao, Z., Luo, D. "Comparative study on removal of metallurgical silicon impurities by different acid leaching methods", Physicochemical Problems of Mineral Processing, 59(2), 162331, 2023. https://doi.org/10.37190/ppmp/162331

[40] Hariani, P. L., Riyanti, F., Desneli, Fatma, Yunita, S., Said, M. "Effect of Calcination Temperature on the Synthesis of Silica from Bagasse", The Journal of Pure and Applied Chemistry Research, 10(2), pp. 140–147, 2021. https://doi.org/10.21776/ub.jpacr.2021.010.02.587

[41] Yu, K., Liu, Y., Yang, Y. "Enhanced thermal properties of polyethylene glycol/modified rice husk ash eco-friendly form-stable phase change material via optimizing support pore structure", Journal of Energy Storage, 43, 103172, 2021. https://doi.org/10.1016/j.est.2021.103172

[42] Supiyani, Agusnar, H., Sugita, P., Nainggolan, I. "Preparation sodium silicate from rice husk to synthesize silica nanoparticles by sol-gel method for adsorption water in analysis of methamphetamine", South African Journal of Chemical Engineering, 40, pp. 80–86, 2022. https://doi.org/10.1016/j.sajce.2022.02.001

[43] Hao, Y., Han, Y., Huang, X., Wang, F., Luo, H. "Research progress of amorphous photonic crystals prepared by self-assembly", Next Materials, 7, 100412, 2025. https://doi.org/10.1016/j.nxmate.2024.100412

[44] Tien Nguyen, G., Van Phuoc, B., Thi Nhung, T., Thi Duy Hanh, L., Tuan, H. N. A., Nhiem, L. T. "Polyethylene Glycol/Rice Husk Ash Shape-Stabilized Phase Change Materials: Recovery of Thermal Energy Storage Efficacy via Engineering Porous Support Structure", ACS Omega, 9(15), pp. 17104–17113, 2024. https://doi.org/10.1021/acsomega.3c09417

[45] Ginting, E. M., Sinulingga, K., Harahap, M. H., Siregar, I. S., Bukit, N. "Analysis of Rice Husk Ash Nanoparticles with Polyethhylene Glycol Surfactants-6000 Using Coprecipitation Method", Chemistry and Materials Research, 8(7), pp. 58–63, 2016.